

## Physical organization of the *ilvEDAC* genes of *Escherichia coli* strain K-12

(isoleucine and valine biosynthesis/restriction endonuclease mapping/heteroduplex analysis/gene expression)

GEORGE M. MCCORKLE, TIMOTHY D. LEATHERS, AND H. E. UMBARGER

Department of Biological Sciences, Purdue University, West Lafayette, Indiana 47907

Contributed by H. E. Umbarger, October 11, 1977

**ABSTRACT** We have determined the physical location of the *ilvEDAC* genes on the restriction cleavage map of the *ilv* region of *Escherichia coli* K-12 by two methods: (i) heteroduplex and endonuclease cleavage analysis of hybrid phages carrying genetically defined parts of the *ilv* cluster and (ii) complementation analysis and enzyme assays to determine *ilv* gene expression from hybrid plasmids containing DNA restriction fragments of the transducing phage  $\lambda$ h80d*ilv*. The *ilvEDA* and *ilvC* operons occupy 2.4 and 0.9 megadalton sequences of DNA, respectively, and are separated by a region of 0.6–0.75 megadalton. The *ilvD* region, specifying dihydroxy acid dehydrase, has a maximum coding capacity of about 55,000 daltons of polypeptide. Our results confirm that *ilvC* is transcribed clockwise on the *E. coli* K-12 map, in the same direction as *ilvEDA*. A secondary  $\lambda$  attachment site within *ilvC* has been located on a small (0.45 megadalton) *EcoRI* fragment. Our results are compared to other physical studies of *ilv* DNA.

The isoleucine and valine biosynthetic enzymes in *Escherichia coli* K-12 are specified by the *ilv* gene cluster represented at 83 min on the linkage map (1). The gene order *E-D-A-C-B*, reading clockwise\* on the map, has long been established (2, 3); *ilvG*, specifying an isoenzyme of the *ilvB* gene product and earlier reported to lie between *ilvE* and *ilvD* (4), was recently shown to lie outside the *ilvEDA* operon (5). The cluster contains four transcriptional units: *ilvEDA* and *ilvB* are repressible, *ilvC* is inducible by its substrate, and *ilvG* is expressed only in certain mutants of K-12 (e.g., *ilvO*<sup>-</sup>). The *ilvEDA* operon is transcribed leftward from *ilvE* to *ilvA* (5–7); *ilvC* is transcribed from the same strand (8, 9) and therefore in the same direction. The direction of transcription of *ilvB* and *ilvG* is not yet known.

A regulatory locus, *ilvO*, has been defined by mutants showing enhanced expression of *ilvEDA* as well as expression of the valine-resistant *ilvG* product. *ilvO* was long thought to lie between *ilvA* and *ilvC* (3, 5) but recent studies on the original “*ilvO*” strains and several newly isolated valine-resistant mutants place this locus between *ilvE* and *rbs* (ref. 6; J. M. Smith, personal communication). The results of Smith *et al.* (5) also suggest that control sites lie promoter-proximal to each gene within the *ilvEDA* operon. Transcripts may or may not be terminated at these sites, depending on specific signals.

One approach to understanding this complex system is to dissect its elements for *in vitro* study and to determine the nucleotide sequences of its regulatory regions for comparison with those of other systems. We report here a physical map of the *ilv* genes that will be useful for locating specific elements and devising strategies for their isolation and purification.

The costs of publication of this article were defrayed in part by the payment of page charges. This article must therefore be hereby marked “advertisement” in accordance with 18 U. S. C. §1734 solely to indicate this fact.

## EXPERIMENTAL PROCEDURES

**Strains, Growth of Bacteriophage and Plasmids, and Purification of DNA.** The *E. coli* K-12 strains have been described (5) or are described in the text. Bacteriophage growth and DNA purification were described (5, 8). Purified unmodified DNA of plasmids pBR313 (10) and pBR322 (11) was a gift of H. W. Boyer, F. Bolivar, and R. B. Meagher. Hybrid plasmids were transformed into the *hsdM*<sup>+</sup> *hsdR*<sup>-</sup> strain JA199 (12) to methylate their DNA before transformation into *hsdR*<sup>+</sup> *ilv*<sup>-</sup> strains. Plasmid DNA was purified as described by Meagher *et al.* (13).

**Restriction Endonuclease Cleavage Analysis.** Endonucleases *EcoRI*, *Bgl* II, *Sal* I, *Hind*III, *Bam*HI, *Sma* I, *Xho* I, *Kpn* I, and *Pst* I were obtained from New England BioLabs, Beverly, MA. Endonuclease digests and agarose and polyacrylamide gel electrophoresis were performed as described (13).

**Heteroduplex Analysis.** Heteroduplexes were prepared by the formamide technique of Westmoreland *et al.* (14) and examined in a Philips EM300 electron microscope. The b519 deletion, estimated as 2.9 kbases by Fianndt *et al.* (15), was used as a single-stranded standard for  $\lambda$ *pilv* phage measurements. S13 RF molecules, used as double-stranded standards in all preparations, were the gift of Ethel Tessman.

**Construction of Hybrid Plasmids.** Endonuclease cleavage fragments of  $\lambda$ h80d*ilv* DNA were covalently inserted into pBR313 or pBR322 by the method of Hersfield *et al.* (16). Recipient strains were transformed essentially by the method of Lederberg and Cohen (17). Recombinant DNA procedures were carried out in a P1 facility (18).

**Expression of *ilv* Genes in Hybrid Plasmid DNA.** *ilv* structural genes in hybrid plasmid DNA were identified by their ability to complement *ilv*<sup>-</sup> strains in medium lacking isoleucine and valine and by assay of enzyme levels in transformed cells, by published methods (19).

## RESULTS

**Physical Characterization of the Bacterial DNA Substitution in  $\lambda$ h80d*ilv*.** Our first objective was to establish a physical map of the *ilv* region. The transducing phage  $\lambda$ h80d*ilv* was our primary source of DNA. This phage had been characterized genetically and physically by LoSchiavo *et al.* (9), who reported that the bacterial substitution carried the *E. coli* K-12 chromosomal region from *rbs* to *cya*, including all of the *ilv* cluster. We determined the size of the substitution in  $\lambda$ h80d*ilv* by

Abbreviation: Md, megadalton.

\* For clarity, clockwise will hereafter be referred to as “leftward” and counterclockwise as “rightward,” as they are oriented in Figs. 1 and 2.

Table 1. Bacterial DNA incorporated in phages studied

	<i>ilv</i> region		Total insertion	
	EM	Gel	EM	Gel
$\lambda$ h80 <i>dilv</i>	—	6.8–7.5	10.0	9.8*
$\lambda$ <i>pilv-lac-1</i>	1.25	0.95–1.35	6.05	6.0†
$\lambda$ <i>pilvA</i>	2.0‡	2.3‡	2.0	2.3
$\lambda$ <i>pilvDA</i>	4.8§	4.5§	4.8	4.5
$\lambda$ <i>pilvEDA</i>	3.3	>3.15	3.3	>3.15

EM, Heteroduplex measurements by electron microscopy; Gel, restriction fragment sizes estimated after electrophoresis in calibrated agarose gels. Measurements are shown in megadaltons (Md); 1.0 kbase = 0.66 Md; 100%  $\lambda$  units = 30.8 Md. Length standards for microscopy were 11.0%  $\lambda$  units for the replicative form of S13 and 50.2%  $\lambda$  for the location of the  $\phi$ 80 attachment site. Measurements do not reflect the revised estimate of  $\lambda$  length (31.8 Md) based on recalculation of the  $\phi$ X174/ $\lambda$  ratio after the  $\phi$ X174 nucleotide sequence was determined. See Fig. 1 legend for description of molecules measured.

\* Includes 3.0 Md or less of non-*ilv* DNA (see Discussion).

† Includes 2.8 Md of *lac* DNA and 2.0 Md of Mu-1(?) DNA.

‡ Includes 0.3 Md of *ilv* DNA to left of  $\lambda$  insertion site.

§ Includes 1.9 Md of *ilv* DNA to left of  $\lambda$  insertion site.

heteroduplex analysis of the DNA of this phage and  $\lambda$ h80 and by mapping the sites cleaved by nine site-specific endonucleases in the DNA of  $\lambda$ h80*dilv* and several other phages and hybrid plasmids containing parts of the *ilv* region. These results are summarized in Table 1 and Fig. 1; a detailed report will be published elsewhere.

**Heteroduplex Structure and Cleavage Analysis of  $\lambda$ *pilv* Phages.** To verify that the F'16 DNA in  $\lambda$ h80*dilv* (20) accurately represented the chromosomal *ilv* region, we analyzed the DNA of a series of genetically characterized phages containing DNA derived directly from the K-12 chromosome,  $\lambda$ *pilvA*,  $\lambda$ *pilvDA*, and  $\lambda$ *pilvEDA*. These had been generated in a single lysate by induction of a strain with  $\lambda$ Y199† inserted at the secondary  $\lambda$  attachment site in *ilvC*, promoter-proximal to the *ilvC44* lesion (5). We also analyzed the DNA of  $\lambda$ *pilv-lac-1*, which carries the *lac* genes fused to *ilvC* and under the control of the *ilvC* regulatory region (21). Fig. 1a shows the structures and endonuclease cleavage sites found in the *ilv* DNA of these phages. Table 1 summarizes the amounts of nonphage DNA contained in each.

The bacterial insertion in  $\lambda$ *pilvDA* exceeded the size of the bacterial substitution in  $\lambda$ *pilvEDA* by about 1.5 megadaltons (Md). Analysis of heteroduplexes revealed that 2.9 Md of the  $\lambda$ *pilvDA* insertion formed a duplex with  $\lambda$ *pilvEDA* bacterial DNA but 1.9 Md did not, suggesting that the latter had come from the *ilvB* side of the insertion site.  $\lambda$ *pilvA* also appeared to contain 0.3 Md or less of DNA from the *ilvB* side.

Endonuclease cleavage analysis confirmed these structures (Fig. 1a). The  $\lambda$  insertion site in *ilvC* was located by the absence of a 0.45-Md *EcoRI* fragment that is near the left end of the bacterial substitution in  $\lambda$ h80*dilv*. The 0.1-Md and 0.75-Md *EcoRI* fragments to its right were found in all three phages.  $\lambda$ *pilvDA*, however, also contained two other *EcoRI* fragments lying to the left of the excision site. A 0.32-Md chromosomal fragment contained the *ilv* site fused to the  $\phi$ 80 left arm in  $\lambda$ h80*dilv*; a 0.5-Md fragment to the left of it on the K-12 chromosome was not present in  $\lambda$ h80*dilv*.

The independently derived  $\lambda$ *pilv-lac-1* contains *ilv* DNA extending from an early site in *ilvC* through the *ilvC* control

† Heteroduplex results demonstrate that our  $\lambda$ Y199 derivatives have an additional 0.24-megadalton deletion contiguous to the b515 deletion and extending toward b519.

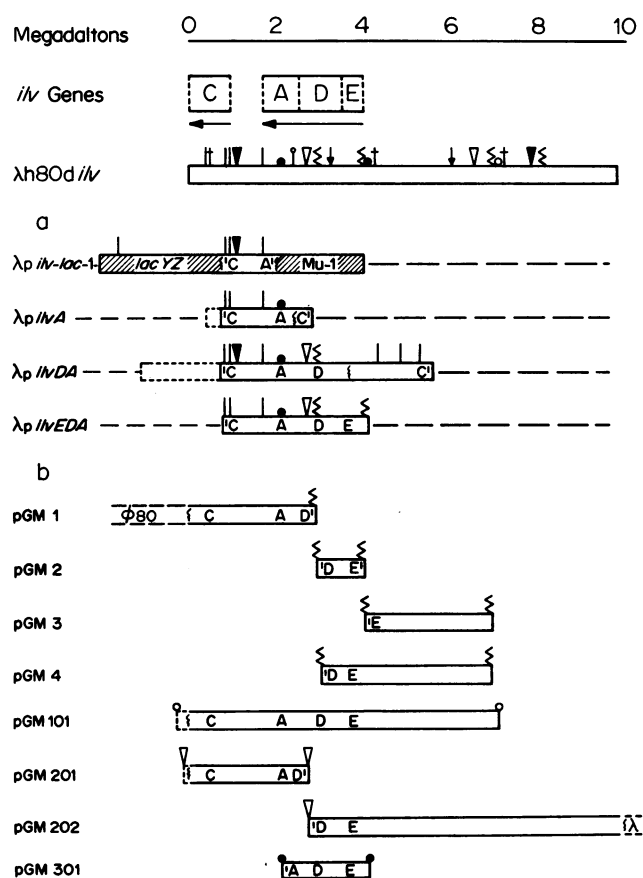


FIG. 1. *ilv* DNA incorporated in hybrid phages and hybrid plasmids. (a) Hybrid phages. Distances are measured in megadaltons from the  $\phi$ 80-bacterial junction of  $\lambda$ h80*dilv*. Measurements were made by electron microscopy of heteroduplexes formed between  $\lambda$ h80*dilv* and  $\lambda$ h80 and between each  $\lambda$ *pilv* phage and  $\lambda$ c1857S7 and by comparative 1% agarose and 7.5% polyacrylamide slab gel electrophoresis after digestion with *EcoRI* (|), *HindIII* (ε), *Pst I* (▽), *Bgl II* (▼), *Sal I* (●), *Sma I* (↓), *Kpn I* (†), *Xho I* (‡), and *BamHI* (○). *ilv* DNA is shown by open bars; non-*ilv* DNA incorporated in  $\lambda$ *pilv-lac-1* is indicated by hatched areas. Fusions joining DNA of different origins are marked by (}).  $\lambda$ *pilvA* and  $\lambda$ *pilvDA* incorporated DNA from both sides of the  $\lambda$  insertion site, resulting in transposition of the *ilvB*-side DNA in the vegetative phage molecules; its actual chromosomal location is shown by dashed bars. Only those  $\lambda$ h80*dilv* cleavage sites actually verified in each  $\lambda$ *pilv* DNA molecule are shown on the  $\lambda$ *pilv* maps; unverified sites are presumed to be present. (b) Hybrid plasmids. Shown are the  $\lambda$ h80*dilv* restriction fragments cloned in pBR313 (pGM1, 2, 3, 4, and 101) and pBR322 (pGM201, 202, and 301). Only terminal cleavage sites are shown; internal sites appear on the  $\lambda$ h80*dilv* map. Complete genes present on a fragment are indicated by letter designation and partial genes present, by a prime sign. Hybrids pGM4 and pGM202 have incorporated partial digest products containing two contiguous uncleaved fragments.

region (21). Cleavage with *EcoRI*, *Bgl II*, and *Sal I* showed that the deletion creating the *lac-ilvC* fusion occurred within the 0.45-Md *EcoRI* fragment and that the rightward 0.1-Md and 0.75-Md *EcoRI* fragments also were present. The *Sal I* site, however, was absent. Therefore, the DNA containing the *ilvC* regulatory region extends at least 0.95 Md but not more than 1.35 Md rightward from the site of fusion with *lac* DNA, in agreement with the heteroduplex results showing that 1.25 Md of *ilv* DNA was incorporated.

These and other results locate the *ilv* site fused to  $\phi$ 80 DNA in  $\lambda$ h80*dilv* and confirm that the 0.45-, 0.1-, and 0.75-Md *EcoRI* fragments are in the same order on the K-12 chromosome and on  $\lambda$ h80*dilv* DNA. They show that the *ilvC* control

Table 2. Complementation of *ilv*<sup>-</sup> strains by hybrid plasmids

Plasmid	Strain and <i>ilv</i> lesion				
	CU424 (C462)	CU406 (A454)	CU534 (D2017)	CU532 (E2050)	CU344 (ΔDAC115)
pGM1	+	+	-	-	-
pGM2			-	-	
pGM3			-	-	
pGM4			-	+	
pGM101	+	+	+	+	+
pGM201	+	+	-	-	-
pGM202		-	-	+	-
pGM301		-	+	+	-

Transformants were selected on Luria plates containing ampicillin (40 μg/ml) or, for cloned *Pst*I fragments, tetracycline (20 μg/ml) and were scored for their *ilv* phenotypes. Complementation by plasmid-carried genes was considered to have occurred when *ilv*<sup>-</sup> cells thus selected showed normal growth within 24–36 hr after restreaking on minimal glucose plates. When only isolated colonies appeared after 48–96 hr, rather than uniform growth, we inferred that recombination had taken place.

region is to the right of the structural gene and that transcription is therefore leftward as it is for *ilvEDA*. Finally, these results locate the λ insertion site and the *lac-ilvC* fusion joint, both early in *ilvC*, near 0.75 Md on our map and place the rightward limits of the *ilvC* control region, *ilvA*, *ilvD*, and *ilvE* at 2.0, 2.5, 3.65, and 4.05 Md, respectively.

***ilv* Gene Expression from Hybrid Plasmids.** We constructed a series of hybrid pBR313 and pBR322 plasmids containing fragments of λh80d*ilv* DNA produced by *Hind*III, *Bam*HI, *Pst* I, and *Sal* I. The *ilv* DNA in these hybrids is shown in Fig. 1b.

The complementation analysis (Table 2) was consistent in all respects with the gene locations indicated by physical analysis of the λ*pilv* phage DNA. Increased enzyme levels were observed in transformed strains in complete accordance with the complementation results. These findings demonstrate which cleavage fragments carry complete coding sequences for each *ilv* gene.

We do not wish to consider now the extent to which *ilv*-specific regulation governs expression of the plasmid-carried genes, because enzyme activity has been determined only under repressing growth conditions, and plasmid copy number per cell has not been independently measured. From comparison of Table 3 and Fig. 1, we believe that message transcripts originated at normal *ilvC* and *ilvEDA* promoters, except in two cases in which *ilvA* was expressed in the absence of the *ilvEDA* promoter. These are the *Hind*III fragment cloned in pGM1 and the *Pst* I fragment in pGM201 and (in opposite orientation) pGM203. Because the Mu-1 polarity studies (5) cited earlier indicate that there is no promoter site preceding *ilvA*, these transcripts probably originated at plasmid promoters or new promoters created by the insertions. The high level of *ilvA* expression in pGM1 is particularly interesting because the *ilv* fragment is inserted in a control region for the pBR313 tetracycline-resistance genes (10), but in the opposite transcriptional orientation.

**Location of *ilv* Genes on the Cleavage Map.** The data shown in Tables 1–3 and summarized in Fig. 1 permit us to correlate *ilv* gene locations with the cleavage map. To facilitate comparison with Fig. 1, we show below, in parentheses, which DNA molecule provides the evidence for each conclusion.

*ilvE* lies leftward of 4.1 Md (pGM301) and 4.05 Md (λ*pilvEDA*). Cleavage at the *Hind*III site at 4.0 Md, however, prevents *ilvE* expression (pGM2, pGM3). The promoter-proximal

Table 3. Enzyme levels in transformed strains

Strain	Plasmid	Relative specific activity			
		IR ( <i>ilvC</i> )	TD ( <i>ilvA</i> )	DH ( <i>ilvD</i> )	TRB ( <i>ilvE</i> )
CU4 ( <i>ilv</i> <sup>+</sup> )	None	1	1	1	1
CU424	None	0	1	1	1
( <i>ilvC462</i> )	pGM1	13	47	1	1
CU532	None	1	3	1	0
( <i>ilvE2050</i> )	pGM4	1	1	0	11
CU406	None	4	0	1	1
( <i>ilvA454</i> )	pGM101	12	43	16	17
CU344	None	0	0	0	1
( <i>ilvDAC115</i> )	pGM201	11	2	0	3
	pGM202	0	0	0	38
	pGM203	19	1	0	3
JA199 ( <i>ilv</i> <sup>+</sup> )	None	1	3	1	2
	pGM301	0	1	53	20

Enzyme names are abbreviated as follows: IR, acetohydroxy acid isomeroreductase; TD, threonine deaminase; DH, dihydroxy acid dehydrase; and TRB, transaminase B. The gene locus specifying each enzyme is in parentheses. Cultures were grown to midlogarithmic phase at 37° in modified Davis and Mingioli minimal glucose medium supplemented with excess isoleucine, valine, and leucine. Enzyme assays were performed by published methods (19). Specific activities were calculated as nmol of product formed per min/mg of protein; they are expressed relative to specific activities of the isogenic prototroph CU4, which were arbitrarily given a value of 1. Actual specific activities in CU4 extracts were: IR, 2.9; TD, 18.2; DH, 10.8; and TRB, 56.0.

terminus of *ilvE* therefore appears to lie between 4.0 and 4.05 Md. The coding sequence of the *ilvE* product, transaminase B, is about 0.55 Md, based on its subunit molecular weight of 30,500 (22) and assuming an average molecular weight of 110 per amino acid residue. The distal terminus, therefore, is estimated to lie at approximately 3.5 Md.

*ilvD* must lie entirely to the left of 3.65 Md (λ*pilvDA*). The cleavage sites at 2.95 Md (pGM1, pGM2, pGM4) and 2.7 Md (pGM201, pGM202) lie within *ilvD* as shown by the data in Tables 2 and 3.

The *ilvA* coding sequence lies entirely to the left of 2.65 Md (λ*pilvA*, pGM1, pGM201) and may lie to the left of 2.45 Md (λ*pilvA* heteroduplex measurement). The cleavage site at 2.1 Md is within *ilvA* (pGM301). The distal terminus of *ilvA* appears to lie to the left of the *Eco*RI site at 1.7 Md; in studies of λ*ilv5*, Collins *et al.* (23) did not detect *ilvA* expression from cloned fragments cleaved at this site. The *ilvA* product, threonine deaminase, requires about 0.9 Md of coding DNA based on its subunit molecular weight of 51,000 (24). These data place *ilvA* somewhere between 1.2 and 2.6 Md; additional data, cited in the Discussion, locate *ilvA* more precisely between 1.55 and 2.6 Md.

For *ilvC*, the secondary λ attachment site located at 0.75 Md lies between the beginning of the *ilvC* coding sequence and *ilvC44*, the most promoter-proximal mutation known in *ilvC*. Preliminary evidence (not shown) indicates that hybrid plasmids that complement *ilvC462* mutants require the 0.1-Md *Eco*RI fragment to the right of the λ insertion site. The beginning of the structural gene therefore probably lies within this fragment. The distal *ilvC* terminus lies to the right of 0.0 Md, because the complete coding sequence is present on pGM201. These limits provide coding space for a polypeptide of molecular weight 50,000, in reasonable agreement with the 57,000 subunit molecular weight of the *Salmonella typhimurium* isomeroreductase subunit (25).

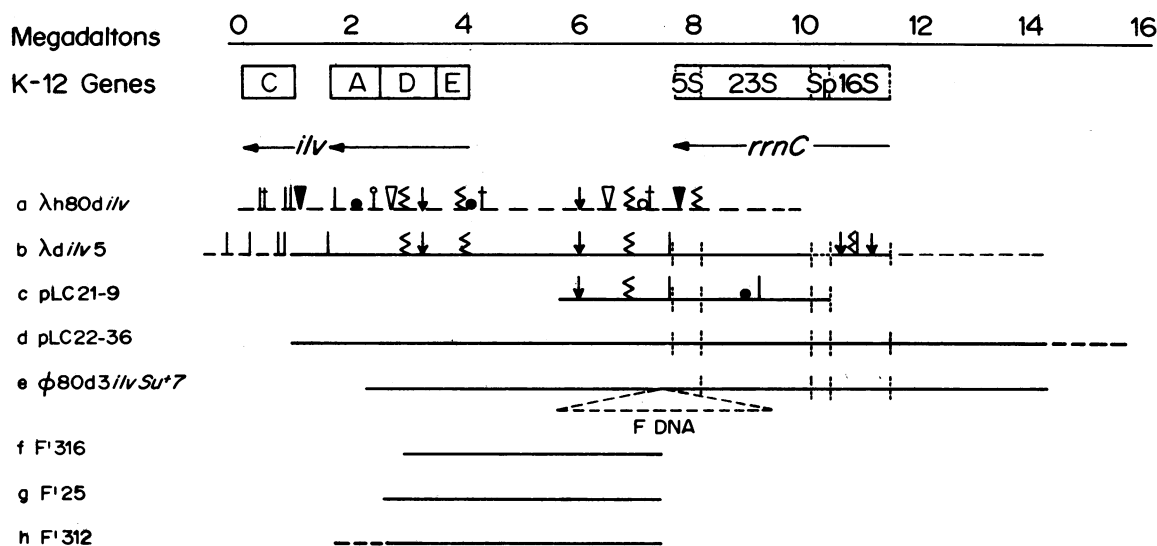


FIG. 2. Comparison of the map of the bacterial DNA substitution in  $\lambda$ h80*dilv* with other physical studies. DNA from the *ilv* region analyzed by others has been aligned with the cleavage map of the *ilv* genes in  $\lambda$ h80*dilv* as follows.

(i)  $\lambda$ h80*dilv*,  $\lambda$ *dilv5*, and pLC21-9 (lines a, b, and c) are aligned by identical cleavage sites of *Eco*RI, *Hind*III, and *Sma* I in their common regions. Cleavage patterns of  $\lambda$ h80*dilv* and  $\lambda$ *dilv5* are not identical to the right of 7.0 Md. Cleavage patterns of  $\lambda$ *dilv5* and pLC21-9 differ to the right of 9.0 Md, presumably because the *rrn* operon carried by  $\lambda$ *dilv5* is a hybrid formed by recombination between the *rrnC* and another unknown *rrn* operon during phage isolation (cf. refs. 23, 26, and 27).

(ii)  $\lambda$ *dilv5* and pLC21-9 have been aligned with each other and with pLC22-36 (line d) and  $\phi$ 80d3*ilvsu*+7 (line e) by electron microscope heteroduplex analysis (26-28) which established the location of *rrn* genes on each.

(iii)  $\phi$ 80d3*ilvsu*+7 has also been aligned (28) with F'316 (line f), F'25 (line g) and F'312 (line h) by the common F-loop marker found in heteroduplexes of these molecules (see line e). Solid lines indicate heteroduplex homology; dashed lines indicate that homology is not known. Arrows show direction of transcription.

## DISCUSSION

We have correlated the locations of four genes of the *ilv* cluster with the cleavage map by two separate methods: physical characterization of transducing phages carrying genetically defined parts of the cluster, and analysis of gene expression from hybrid plasmids carrying restriction fragments of *ilv* DNA. We have also correlated our cleavage map of *ilv* DNA with other physical studies of this region by means of cleavage and heteroduplex homologies, as shown in Fig. 2. All of the data, with one exception discussed below, support the physical map of the *ilvEDAC* genes shown at the top of Figs. 1 and 2.

The locations of *ilvE* and *ilvC* are defined within the narrow limits of 3.5-4.05 and 0.0-0.95 Md, respectively, on our map. The 2.55-Md sequence between these genes has been shown to contain the *ilvC* control region and two cleavage sites each within *ilvA* and *ilvD*. The physical extent of the *ilvC* control region and *ilvD* are not known, but the *ilvA* coding sequence is about 0.9 Md based on the size of its protein product. On the basis of our data alone, *ilvA* could lie anywhere between 1.2 and 2.6 Md on our map. We can refine this estimate, however, from the heteroduplex measurements (29) of F'316 and F'25, which contain genetically defined deletion end points in the promoter-proximal end of *ilvA* and promoter-distal end of *ilvD*, respectively (30). Fig. 2 shows that these end points are located at 2.46 and 2.79 Md on our map. From our measurements of  $\lambda$ *pilvA*, *ilvA* lies to the left of 2.6 Md. The promoter-distal terminus of *ilvA* thus appears to lie between 1.56 and 1.7 Md.

With *ilvA* located, it is evident that an interoperon region of 0.6-0.74 Md lies between *ilvC* and *ilvA*. This entire region as well as the distal half of *ilvA* was acquired by  $\lambda$ *pilv-lac-1*, which was selected for the presence of the *ilvC* control region. We cannot yet say whether all or merely a portion of the region

comprises *ilvC* regulatory DNA, or whether the presence of the distal *ilvA* sequence is significant.

The *ilvD* region, to the right of *ilvA*, occupies 0.9-1.06 Md of DNA, sufficient to specify 50,000 daltons or more of polypeptide. We do not know the extent of untranslated sequences flanking *ilvD* nor the size of the coding sequence for the *ilvD* product, dihydroxy acid dehydrase. Two cleavage sites within *ilvD* have been identified in the left end of this region, but we have not yet been able to determine whether cleavage in the *ilvE*-proximal part of the region interferes with *ilvD* function. It is possible, although we think unlikely, that an additional unidentified protein might be coded here. Polarity studies (5), however, exclude the possibility that *ilvG* lies within this region.

**Comparison of Bacterial Region of  $\lambda$ h80*dilv* with Other Studies.** As shown in Fig. 2, other physical studies of *ilv* DNA can now be related to our map of the bacterial substitution in  $\lambda$ h80*dilv*. Several points emerge from these comparisons.

(i) The cleavage maps of  $\lambda$ h80*dilv* and  $\lambda$ *dilv5* are identical from 0.0 Md at least to 6.85 Md and possibly to 7.46 Md, where F DNA fuses with *ilv* DNA in F'14 and its F' derivatives. To the right of this point,  $\lambda$ *dilv5* contains a hybrid *rrn* operon (see Fig. 2 legend). The cleavage pattern beyond 7.46 Md shows that  $\lambda$ h80*dilv* contains different DNA of undetermined origin.

(ii) The cleavage homology of  $\lambda$ h80*dilv* and  $\lambda$ *dilv5* and the heteroduplex homology of the latter with plasmid pLC22-36 (26) show that  $\lambda$ h80*dilv* DNA is identical with the chromosomal DNA in pLC22-36 in their common regions, to the extent that this can be determined by these methods. This comparison also establishes the distance between the end of the 5S RNA gene in *rrnC* and the beginning of *ilvE* as approximately 3.3 Md.

(iii) As noted above, the heteroduplex measurements of F'316 and F'25 (29), as aligned on our map in Fig. 2, are in excellent

agreement with the locations we have determined for *ilvD* and *ilvA*. However, the location of the F'312 end point, which lies distal to the *ilvC44* lesion (6, 30), does not agree with our evidence for the location of *ilvC44*. We place *ilvC44* to the left of the secondary  $\lambda$  attachment site at 0.75 Md, at least 1.75 Md from the distal terminus of *ilvD*. Lee *et al.* (29) found the F'316 and F'312 end points to be 1.15 Md apart. We are unable to suggest an explanation for this discrepancy.

Our results may also be compared with those of LoSchiavo *et al.* (9), who concluded that *ilvB* and *cya* are present on  $\lambda$ h80*dilv* DNA. We have been unable to confirm their results by genetic analysis in our laboratory, either for  $\lambda$ h80*dilv* or for F'16 from which it presumably was derived (J. M. Smith, personal communication). The bacterial substitution in  $\lambda$ h80*dilv* ends immediately to the left of the *ilvC* structural gene. Because both *ilvB* and *cya* lie to the left of *ilvC* on the genetic map, we conclude that neither is present on  $\lambda$ h80*dilv*. We cannot yet determine the physical location of *ilvG* from our data; this question may be clarified by mRNA-DNA hybridization studies and by experiments designed to detect expression of *ilvG* by read-through from plasmid promoters.

We thank Drs. Richard B. Meagher, Francisco Bolivar, and Herbert W. Boyer for plasmid-containing strains, purified plasmid DNA, and assistance with molecular cloning techniques; Dr. Ethel Tessman for invaluable help in developing heteroduplex techniques; and Dr. John M. Smith for fruitful discussions and permission to report his unpublished observations. David M. Miller's skilled technical assistance was indispensable. The work was supported by National Institutes of Health Regulation Training Grant 5 T32 GM07076 and Research Grant 5 RO1 GM12522 from the National Institute of General Medical Sciences.

1. Bachmann, B. J., Low, K. B. & Taylor, A. L. (1976) *Bacteriol. Rev.* **40**, 116-167.
2. Ramakrishnan, T. & Adelberg, E. A. (1965) *J. Bacteriol.* **89**, 661-664.
3. Ramakrishnan, T. & Adelberg, E. A. (1965) *J. Bacteriol.* **89**, 654-660.
4. Favre, R., Wiater, A., Puppo, S., Iaccarino, M., Noelle, R. & Freundlich, M. (1976) *Mol. Gen. Genet.* **143**, 243-252.
5. Smith, J. M., Smolin, D. E. & Umbarger, H. E. (1976) *Mol. Gen. Genet.* **148**, 111-124.
6. Cohen, B. M. & Jones, E. W. (1976) *Genetics* **83**, 201-225.
7. Childs, G., Ohtsubo, E. & Freundlich, M. (1976) *Abstracts, ICN-UCLA Winter Conference on Molecular Mechanisms in the Control of Gene Expression*, Abstract no. 111.
8. Vonderhaar, R. A. & Umbarger, H. E. (1974) *J. Bacteriol.* **120**, 687-696.
9. LoSchiavo, F., Favre, R., Kasai, T., Cascino, A., Guardiola, J., Caro, L. & Iaccarino, M. (1975) *J. Mol. Biol.* **99**, 353-368.
10. Bolivar, F., Rodriguez, R. L., Betlach, M. C. & Boyer, H. W. (1977) *Gene* **2**, 75-93.
11. Bolivar, F., Rodriguez, R. L., Greene, P. J., Betlach, M. C., Heyneker, H. L., Boyer, H. W., Crossa, J. H. & Falkow, S. (1977) *Gene* **2**, 95-113.
12. Ratzkin, B. J. & Carbon, J. (1977) *Proc. Natl. Acad. Sci. USA* **74**, 487-491.
13. Meagher, R. B., Shepherd, R. J. & Boyer, H. W. (1977) *Virology* **80**, 362-375.
14. Westmoreland, B. C., Szybalski, W. & Ris, H. (1969) *Science* **163**, 1343-1348.
15. Fiant, M., Hradecna, Z., Lozeron, H. A. & Szybalski, W. (1971) in *The Bacteriophage Lambda*, ed. Hershey, A. (Cold Spring Harbor Laboratory, Cold Spring Harbor, NY), pp. 329-354.
16. Hershfield, V., Boyer, H. W., Yanofsky, C., Lovett, M. A. & Helinski, D. R. (1974) *Proc. Natl. Acad. Sci. USA* **71**, 3455-3459.
17. Lederberg, E. M. & Cohen, S. N. (1974) *J. Bacteriol.* **119**, 1072-1074.
18. U.S. Department of Health, Education, and Welfare (1976) *National Institutes of Health Guidelines for Recombinant DNA Research* (National Institutes of Health, Publication no. [NIH] 76-1138), Vol. 1.
19. Kline, E. L., Brown, C. S., Coleman, W. G., Jr. & Umbarger, H. E. (1974) *Biochem. Biophys. Res. Commun.* **57**, 1144-1151.
20. Avitabile, A., Carlomagno-Cerillo, M. S., Favre, R. & Blasi, F. (1972) *J. Bacteriol.* **112**, 40-47.
21. Smith, J. M. & Umbarger, H. E. (1977) *J. Bacteriol.*, **132**, 870-875.
22. Monnier, N., Montmitonnet, A., Chesne, S. & Pelmont, J. (1976) *Biochimie* **58**, 663-675.
23. Collins, J., Fiil, N. P., Jørgensen, P. & Friesen, J. D. (1976) in *Control of Ribosome Synthesis, Alfred Benzon Symposium IX* (Munksgaard, Copenhagen), pp. 356-369.
24. Calhoun, D. H., Rimerman, R. A. & Hatfield, G. W. (1973) *J. Biol. Chem.* **248**, 3511-3516.
25. Hofler, J. G., Decedue, C. J., Luginbuhl, G., Reynolds, J. A. & Burns, R. O. (1975) *J. Biol. Chem.* **250**, 877-882.
26. Kenerley, M. E., Morgan, E. A., Post, L., Lindahl, L. & Nomura, M. (1977) *J. Bacteriol.*, **132**, 931-949.
27. Morgan, E. A., Ikemura, T. & Nomura, M. (1977) *Proc. Natl. Acad. Sci. USA* **74**, 2710-2714.
28. Ohtsubo, E., Soll, L., Deonier, R. C., Lee, H. J. & Davidson, N. (1974) *J. Mol. Biol.* **89**, 631-646.
29. Lee, H. J., Ohtsubo, E., Deonier, R. C. & Davidson, N. (1974) *J. Mol. Biol.* **89**, 585-597.
30. Marsh, N. J. & Duggan, D. E. (1972) *J. Bacteriol.* **109**, 730-740.